Carbohydrate Research, 160 (1987) 227–241
Elsevier Science Publishers B V , Amsterdam – Printed in The Netherlands

THE CONCENTRATION DEPENDENCE OF THE SEDIMENTATION RATE OF AMYLOSE, CELLULOSE, AND DEXTRAN IN AQUEOUS SOLUTION

HANS ELMGREN
Institute of Physical Chemistry, Uppsala University, P O. Box 532, S-751 21 Uppsala (Sweden)
(Received March 5th, 1986, accepted for publication in revised form, July 20th, 1986)

ABSTRACT

The polymers amylose, cellulose, and dextran are compared with regard to their conformation. The comparison is based on a combination of sedimentation and electron-spin resonance or fluorecence-depolarization data according to a theory developed for the sedimentation of polymer coils. The comparison shows that the amylose coils are built up from heavy, compact segments (presumably helices). Cellulose coils consist of heavy, expanded segments. Dextran coils are flexible. These findings are not new. The advance made with the theory presented is that it gives a new way to determine the chain stiffness. Another advance is that it makes the extrapolation for s_0 more precise; it is demonstrated for the case of cellulose in the solvent Cadoxen. A new picture of the molecular mass dependence on s_0 is obtained thereby. From measured relations between the solvent mobility and the concentration, it is possible to calculate how the solvent mobility changes with the distance from a polymer segment (the mobility profile). A method for such calculations is described. The mobility profiles in the systems studied are shown, together with that of polystyrene in a theta-solvent.

THEORY

According to classical sedimentation theory[1], the relation between the sedimentation coefficient s and the friction coefficient f of a sedimenting species is

$$s = s_0(f_0/f) \qquad (1)$$

where the index zero refers to zero concentration conditions. The relation is based on the balance of the driving force (which is proportional to the effective mass) and the friction force (which is the friction coefficient times the sedimentation rate of solute through the solvent). The observed (normalized) sedimentation rate s is measured with the cell as reference. The sedimenting volume forces solvent upwards[2]. The speed which gives rise to the friction force is thus higher than s, except at zero concentration.

0008-6215/87/$ 03 50

The concentration dependence of s is usually given through that of f as $f = f_0(1 + kc + \ldots)$. These relations were developed for the case of compact macromolecules (*i.e.*, solid particles, impenetrable for the solvent) in dilute solutions. They have also been used in studies of polymer coils at high concentrations. In such cases, Eq. *1* turns out to be insufficient. The complex concentration dependence, as hidden in f, will make the relation rather academic, except for the cases when $c \sim 0$. In more modern theories (scaling laws[3]), s is assumed to be proportional to certain powers of the polymer concentration. This method has not been successful either. The main reason for these difficulties is that the solvent can, with some resistance, drain through the polymer coils[4].

The classical model[5] for dilute polymer solutions describes the macromolecules as swollen polymer coils, well separated in bulk solvent. On an average, the coils are nearly Gaussian[6], *i e.*, they are describable basically by random-flight statistics[7] Accordingly, they can be regarded as N_s straight segments, each containing n_s monomers such that $N_s \cdot n_s$ = d.p., the degree of polymerization of the polymer[8]. The segment concentration is highest in the center, and fades out approximately as the Gaussian curve moves outwards. At any distance from the center, the segment concentration increases monotonically with d.p. However, the total volume of the coil increases faster than the d.p. Therefore, increasing d.p. results in a decrease in the average segment concentration in the coils. The hydrodynamic average segment concentration inside the coils is $c^* = 1/[\eta]$, where $[\eta]$ is the intrinsic viscosity[9,10]. The analogous value on the volume fraction scale is $\phi^* = 1/[\eta]_\phi$, where $[\eta]_\phi$ is the limiting value of η_{red}/ϕ when ϕ approaches zero (With matching units, $\phi = c \cdot \bar{v}_2$, where $\bar{v}_2$ is the partial specific volume of the solute. Knowing it, one can thus freely alternate between the two scales for the solute concentration.)

From the classical model for polymer solutions, it follows that the solvent in a dilute solution belongs partly to an intraphase (inside the coils), and partly to an inter-phase (between the coils). As long as the coils are well separated, an addition of polymer to the solution will not affect the concentration c^* in the intraphase. It only results in an increase in the number of coils, and thus, in the fraction Ψ of the solvent which belongs to the intraphase

Sedimentation can be seen as being a process in which solvent passes the solute in an upward stream. In the case of polymer solutions, there will be two streams: one with a "coil-solvent" speed in the interphase, and another, with a "segment-solvent" speed, in the intraphase In dilute solutions, the concentration dependence of the average speed s is, therefore, a question of the partition of solvent between the inter- and the (retarded) intra-phase.

When the overall concentration c approaches c^*, the interphase gradually disappears A further increase in concentration then corresponds to an increased segment concentration, which is statistically homogeneous throughout the sample. Not until now are all solvent molecules exposed to the same speed relative to the solute. This speed is the sedimentation rate of the polymer segments. Both the driving and the friction forces are now proportional to the chain length. Therefore,

the sedimentation rate is d.p.-independent in the concentrated regime.

In a series of articles[11–14], this was penetrated more in detail. The resulting relation corresponding to Eq. *1* is

$$\frac{s}{1-\phi} = \Psi S_0(\langle m_1\rangle_{\text{intra}} - m_s) + (1-\Psi)s_0\langle m_1\rangle_{\text{inter}}, \tag{2}$$

where ϕ is the volume fraction of the polymer in the solution. The denominator $(1-\phi)$ transforms s to the solvent-fixed reference frame. S_0 is a d.p.-independent constant, related to the sedimentation rate of the segments, $\langle m_1\rangle_i$ is the solvent mobility in the phase as indicated, and m_s is the segment mobility. It is a correction for counter diffusion of segments during the sedimentation. In the case of flexible polymers, this effect is often significant. (In the second term, a corresponding correction could be made for the counter diffusion of coils.) All mobilities are normalized by means of the mobility of the solvent molecules in bulk solvent. They thus have a common reference, which makes them commensurable. The value of $\langle m_1\rangle$ is measurable as η_0/η, where η is the microviscosity of the solvent. It can be determined experimentally, *e.g.*, by the electron-spin resonance or the fluorescence-depolarization technique.

In the case of compact macromolecules, $\Psi = 0$, and Eq. *2* is equivalent to Eq. *1* over the entire concentration range. In the case of permeable coils at concentration above c^*, $\Psi = 1$, and Eq. *2* is reduced to

$$\frac{s}{1-\phi} = S_0(\langle m_1\rangle - m_s), \tag{3}$$

which is of the same type as Eq. *1*. Rearrangement of Eq. *3* gives

$$\langle m_1\rangle = m_s + \frac{1}{S_0}\cdot\frac{s}{1-\phi}. \tag{4}$$

Thus, if $\langle m_1\rangle$ *versus* $s/(1-\phi)$ gives a straight line, S_0 and m_s can be obtained from the slope and the intercept. Because the self-diffusion coefficient of the segments is governed by their effective mass, the value of m_s is a measure of the chain flexibility. S_0 gives direct information about the frictional properties of the monomers in the chain, and is a useful tool in comparative studies of polymers. Besides this combination method to obtain S_0, there is another direct way. As $S_0 = s$ under free-draining conditions, it is directly measurable on polymers of low d.p. This is especially the case when the polymer coils are strongly expanded. Except for end effects, s_0 should then be d.p.-independent over a certain d.p. range The larger the number n_s of monomers per segment, the wider is this range

At very low polymer concentrations, Eq. *2* approximates to

$$s = \Psi S^* + (1-\Psi)s_0, \tag{5}$$

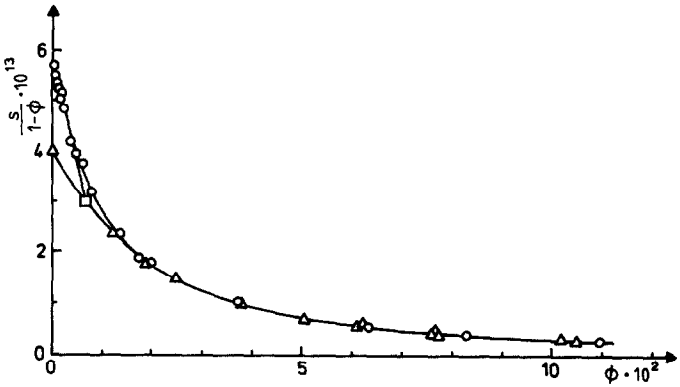

Fig 1 Amylose in water. [Key Circles. the sedimentation coefficients $s/(1 - \phi)$ (solvent-fixed reference frame) *versus* the volume fraction, ϕ, of the polymer in the solution. Triangles: solvent mobility data, as determined by means of electron-spin resonance[15] Square· the point (ϕ^*,S^*), corresponding to the sedimentation rate of segments at the average volume fraction, ϕ^* (= $1/[\eta]_\phi$), of the segments in the coils.]

where $S^* = S_0(\langle m_1 \rangle_{\text{intra}} - m_s)$ is a constant, due to the constancy in c^*. According to this relationship, s varies linearly with Ψ (and thus with the concentration) from s_0 (at $c = 0$) toward S^* (at $c = c^*$). In the work cited, this statement was verified for all polymer systems studied. In Fig. 1, it is shown for amylose in water[15]. The square refers to the point (c^*,S^*). As S^* and c^* are measurable, they can give very strong guidance in the extrapolation for s_0. (From this it also follows that $1/s$ is not linearly dependent on the concentration. Thus, it is not appropriate to use linear extrapolations for $1/s_0$). The initial linearity in s with c explains why scaling is impossible unless the d.p. is infinite. In such cases, however, c^* is zero, s_0 will be underestimated, and Eq. *3* is valid over the entire concentration region. Thereby, scaling is likely to be done more easily.

All parameters in Eq. *2* have physical significance, and they are measurable. Combined measurements on several polymer systems[11–15] have shown that the equation is a close description of the concentration dependence of s. In other words, the systems tested behave just as expected. The use of (relative) mobilities instead of (relative) friction coefficients emanates from the view of sedimentation as the motion of solvent relative to the polymer segments. According to this view, the sedimentation rate is determined by the ability of the solvent to pass the coils.

It is now possible to take one step further. The concentration dependence of $\langle m_1 \rangle$ can be transformed into a mobility profile[16] which describes how the local solvent mobility (m_1) changes with the distance b from the surface of the polymer segment. (The measured solvent mobility $\langle m_1 \rangle$ is the average of m_1 over the whole solvent volume, and the polymer concentration c is a measure of the average distance between the polymer segments.) The profile can be described by the relations

$$m_1 = m_s + (1 - n_s)m_{1,0} \tag{6}$$

and

$$m_{1,0} = 1/[1 + (a/b)^n], \tag{7}$$

where $m_{1,0}$ is the solvent mobility in a segment-fixed reference frame, a is a "shell thickness" constant, and n is a constant determined by the character of the profile. Eq 7 describes the influence from one segment, at infinite distance from others. The simultaneous perturbation from several segments is accounted for by replacing $(a/b)^n$ with the sum $\Sigma_i(a/b_i)^n$ in the denominator. The index refers to segment i

Comprehensive calculations (by means of numerical integration of $m_{1,0}$ over 15,625 volume elements, taking 42 cylindrical, three-dimensionally oriented segments into account, $\langle m_1\rangle_0$ was computed for broad intervals of ϕ, a, and n) showed that the mobility profile is accessible from measurable data by means of the relations

$$\langle m_1\rangle_0 = \frac{\langle m_1\rangle - m_s}{1 - m_s} = \frac{1}{1 + (\alpha/\beta)^\nu} \tag{8}$$

and

$$\beta/r = (1.21/\phi)^{1/2} - 1. \tag{9}$$

where r is the segment radius, and α and ν are constant over the entire concentration range $\phi \leq 0.5$. These constants have the following relation to a and n:

$$a/r = 0.19 \cdot \nu \cdot \alpha/r \tag{10}$$

$$n = \nu \cdot \left(1 + 0.27\left(\frac{\nu}{\alpha/r}\right)^2\right). \tag{11}$$

Rearrangement of Eqs. 8 and 9 gives

$$\log(\langle m_1\rangle_0^{-1} - 1) = \nu \log\alpha/r - \nu \log\beta/r. \tag{12}$$

Thus, the measurable quantity $\log(\langle m_1\rangle_0^{-1} - 1)$ is linearly dependent on $\log[(1.21/\phi)^{1/2} - 1)]$. The parameters ν and α/r are obtained from the slope and the intercept in such a plot. By means of Eqs. 10 and 11, a/r and n can now be determined. If the segment radius r is known, it is thus possible to calculate the mobility profile. (Corresponding calculations were also performed for the cases of spherical macromolecules and, in separate work[17], parallel plates.)

Some very important observations were made in the work cited. One is that plots according to Eq. *12* were always linear when $n \leq 3$, but curved when $n = \infty$. (The latter corresponds to an immobile solvent shell with thickness a, surrounded by unperturbed solvent.) Thus, it is easy to distinguish between smooth and stepwise changes of the solvent mobility around polymers. Another observation was that the computed values of $\langle m_1 \rangle_0$ are insensitive for inhomogenities in the spatial distribution of the segments. The linearity of the plot is maintained far down in the dilute regime, where the segments occur in well separated coils (clusters). As long as $n \leq 3$, the linearity is reliable to such an extent that it can be used as a control of the measured data on $\langle m_1 \rangle$. Theoretically, it could also be used for the determination of m_s and S_0 directly from sedimentation data.

A third observation was that a/r is the independent "shell thickness" parameter. The solvent is thus perturbed over a distance that is proportional to the radius of the solute, independent of type (cylinder or sphere). This is in line with Stokes' law.

The knowledge of the mobility profile should make new steps possible. One would be to calculate how the hydrodynamic radius of a polymer coil depends on d.p. Another step would be to relate the mobility profile parameters to the thermodynamic properties of the polymer system. However, such steps are beyond the scope of the present article. Instead, it is shown here how the relations presented are used in a comparative study of amylose, cellulose, and dextran. Especially, their m_s, S_0, and mobility profiles are compared.

Concentrated solutions

Fig. 2 shows how the sedimentation rate depends on the volume fraction ϕ in the case of [weakly *O*-(2-hydroxyethyl)ated] amylose, *O*-(2-hydroxyethyl)cellulose

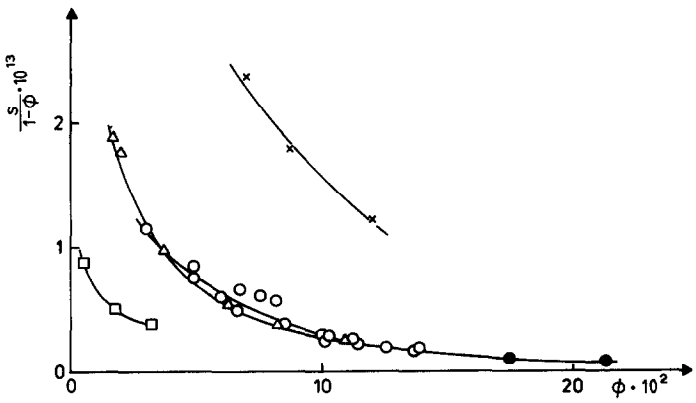

Fig 2 The sedimentation coefficient $s/(1 - \phi)$ (solvent-fixed reference frame) *versus* the volume fraction, ϕ, of polymers at high concentrations ($\phi > 2\ \phi^*$). [The systems are, polystyrene in cyclopentane[25] (crosses), amylose in water[15] (triangles), dextran in water[14,26] (circles), and HEC in water[27] (squares) The two filled dextran circles correspond to those in Figs 4 and 5]

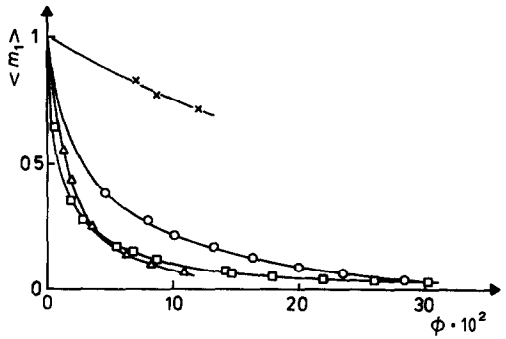

Fig 3 The average solvent mobility $\langle m_1 \rangle$ *versus* the volume fraction ϕ of the polymer in solution. [N.m r data on polystyrene in cyclopentane[28] (crosses), f d p data on dextran in water[14] (circles), e s r data on amylose in water[15] (triangles), and f d.p data on HEC in water[29,30] (squares)]

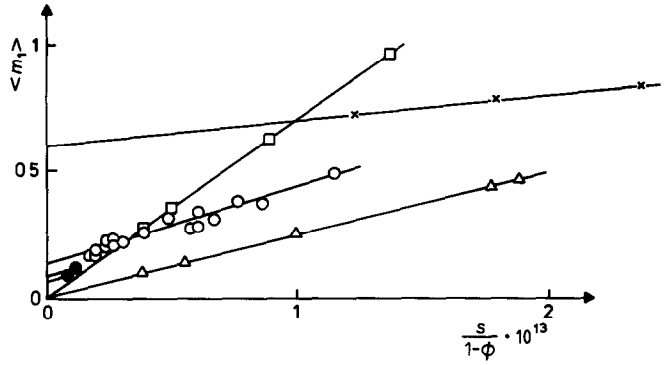

Fig. 4 Plot according to Eq *4* for the determination of m_s and S_0 For symbols, see Fig 2

(HEC), and dextran in water. Data on polystyrene (p.s.) in cyclopentane are alo shown, for comparison. All data refer to the concentrated regime ($\phi > 2\phi^*$). Fig. 3 demonstrates the change in $\langle m_1 \rangle$ with concentration for the same systems.

In Fig. 4, the data are combined in a plot according to Eq. *4*, giving m_s and S_0 as shown in Table I. (The values of m_s and S_0 thus obtained were used in Fig. 1, where the circles correspond to the left-hand side in Eq. *3*, and the triangles correspond to the righ-hand side.) As the molar mass M_s of a segment should be proportional to m_s^{-2} (which is a thermal equilibrium condition according to Boltzmann), the m_s values in Table I confirm earlier experience that amylose and HEC are stiff, as compared with dextran. According to the dextran data in Fig. 4, m_s decreases with increasing concentration at very high concentrations. (S_0 is a constant, and thereby also the slope of the dextran extrapolations) This decrease was to be expected.

The S_0 values in Table I hide some valuable information. In the case of HEC, dextran, and p.s., a stronger concentration dependence on $\langle m_1 \rangle$ is accompanied by a lower value of S_0, exactly as expected: high friction leads to slow motion. How-

TABLE I

SEDIMENTATION AND MOBILITY PROFILE PARAMETERS

Polymer	m_s	n_s	$S_0 \cdot 10^{13}$ (s)	$\bar{\nu}_2$ (mL/g)	$\frac{S_0 \eta_1{}^a}{1 - \bar{\nu}_2 \rho_1}$	*Mobility profile parameters*			
						n	a/r	r (Å)	a (Å)
Amylose	0	∞	4 05	0 60	10 2	2 25	3 24	6 5	21
HEC	0	∞	1 4	0 70	4 7	1 61	2 92	3	8 8
Dextran	0 14	1 9	3 4	0 60	8 5	2 29	2 79	3	8 4
P s in cyclopentane at 40°	0 6	0 6	10	0 94	17	3 2	1 3	4	5 2

[a]The segment sedimentation coefficient S_0, as normalized with respect to the solvent viscosity η_1 and the bouyancy

ever, amylose does not follow this scheme. Even though it shows as high a friction as does HEC, it has the highest S_0 value of the three polysaccharides. This is reasonable only if the amylose segments have a more compact structure than the others. For several reasons, it can be assumed that this is the case, and that the compact structure is a helix[15,18].

Knowing the m_s values, $\langle m_1 \rangle_0$ values were calculated according to Eq. *8*. The

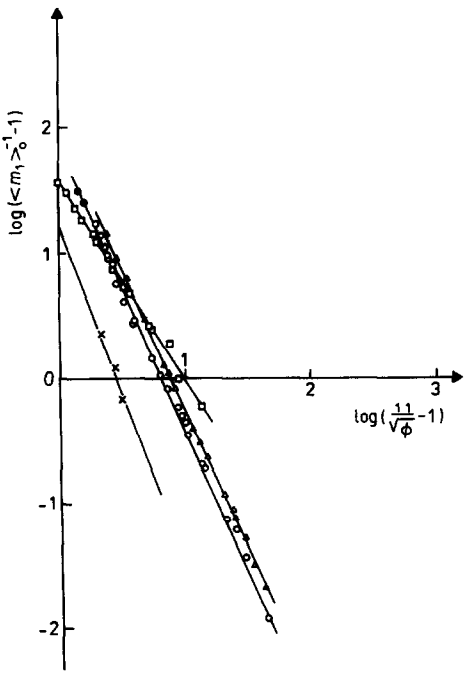

Fig 5 Plot according to Eq *12* for the determination of the mobility profiles of water around amylose (triangles), HEC (squares), and dextran (circles), and of cyclopentane around polystyrene (crosses) Filled circles see Fig 2

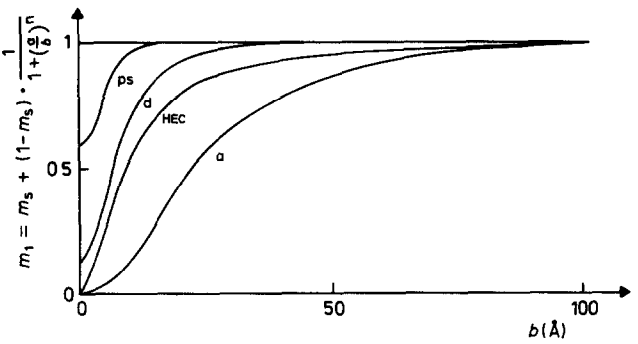

Fig 6 The mobility profiles around polystyrene (p s), dextran (d), HEC, and amylose (a)

values thus obtained were plotted according to Eq. *12*. As may be seen in Fig. 5, the plots are linear over the entire concentration range. In the case of amylose and dextran, the linearity is verified over more than two orders of magnitude in the polymer concentration. The fact that the linearity is maintained for dextran at the two highest concentrations (the two filled circles to the very left in the plot) is a double check that m_s really decreases with increasing concentration, as was found in Fig. 4. If this decrease were not considered, a dextran line would be obtained which would bend significantly upwards in Fig. 5.

From slopes and intercepts in Fig. 5, the mobility profile parameters a and n were obtained. Their values are given in Table I. The corresponding mobility profiles are shown in Fig. 6. As may be seen there, the profiles are very like in character, but very different in perturbation distances. As compared with the polysaccharides, p.s. perturbs cyclopentane very little. The perturbation of the polysaccharides on water is very strong. This is especially the case for amylose, which reduces the mobility of the surrounding water by ten percent as far out as 50 Å from the segment surface. (The profile was calculated using $r = 6.5$ Å, which is the radius of the assumed amylose helix[19].)

Dilute solutions

The overwhelming part of all sedimentation studies reported is concerned with dilute solutions. Not until the latest decades was the concentration dependence of s of any interest, except for its role in the extrapolation to s_0. In the case of compact macromolecules, the extrapolation was sometimes made of s, but preferentially of $1/s$. The latter method was transmitted also to measurements on polymer coils. As already shown, this is not satisfactory. A linear plot of s is to be preferred. If the "square point" (see Fig. 1) is known, it can be used as a starting point for the extrapolation The s_0 value obtained will then be more accurate than that obtained from the sedimentation data only. However, there is a problem connected with the linear extrapolation of s from the point (c^*,S^*). The local segment concentration in the coil center is much higher than the average concentration c^*.

Because the center concentration increases, and c^* decreases, with increasing d.p., the difference between them will increase rapidly with d.p. The problem arises when the segment mobility $m_s > 0$ and is concentration-dependent. In such cases, S^* will be larger than expected. This is striking in the case of very flexible coils of high d.p. and low expansion, such as high-molecular-weight polystyrene in theta-solvent. In the case of polysaccharides the effect is small (dextran) or nil (amylose

TABLE II

CELLULOSE IN CADOXEN[a]

Cellulose sample	$d\,p_{ww}$	$\phi^* \cdot 10^3$	$\phi \cdot 10^3$	$s \cdot 10^{13}$ (s)	$s_0 \cdot 10^{13}$ (Henley)	$s_0 \cdot 10^{13}$ (Fig 7)
L1 ●	4600	0 456	0.271	3.46	5 49	5.90
			0 284	3 39		
L3 ○	2680	0 710	0.258	3 22	4 53	4.45
			0 323	3 09		
			0.374	2 87		
L7 ○	1700	1.00	0 445	2.56	3.80	3.40
			0.587	2.29		
L8 ▲	1280	1 17	0.310	2.59	3.17	3.05
			0.445	2.46		
			0.542	2.24		
			0.542	2 21		
L9 △	950	1.45	0.342	2 45	2 75	2.65
			0.419	2 09		
			0.490	2 29		
			0.600	2 01		
			0 632	2 03		
			0 697	1 94		
L10 **X**	260	4 39	0 684	1 62	1 80	1.70
			0.735	1 53		
			0.890	1 46		
			1.039	1.41		
			1 232	1 39		
			1.503	1.33		

[a]Excerpt from ref 20, and s_0 values, as obtained in Fig 7 Symbols in the cellulose sample column correspond to those in Figs. 7 and 8

TABLE III

SEGMENT SIZES AS DETERMINED FROM AVERAGE SEGMENT CONCENTRATIONS ϕ^* IN COILS WITH d p. = 2000

Polymer	*Solvent*	ϕ^*	$l_m/\text{Å}$	$n_s \cdot \alpha^2$
P s	θ-solvent	0.032	3	5.5
Dextran	water	0 014	6	2 4
Amylose	water	0 008	1 3	74
Cellulose	Cadoxen	0 001	5	20[a]
HEC	water	0 001	5	20[a]

[a]Assumed value.

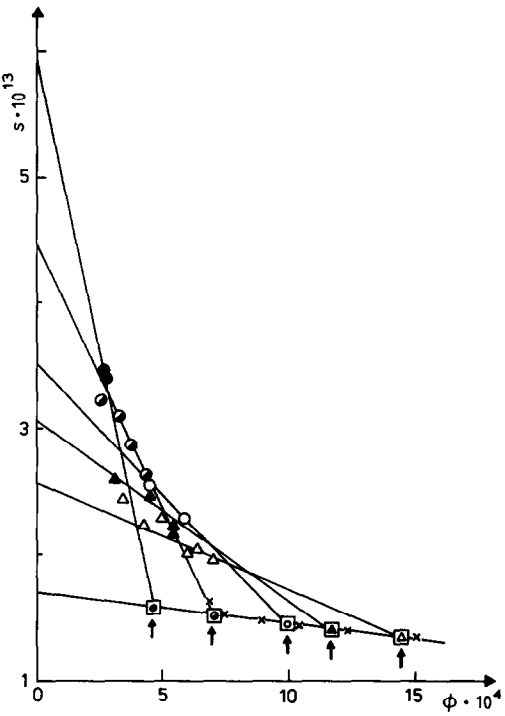

Fig 7 The sedimentation coefficient of cellulose in Cadoxen *versus* the volume fraction of the polymer. [Data from ref 20 (they are also given in Table II) Different symbols for different molecular masses (see Table II) The squares correspond to $\phi = \phi^*$ (= $1/[\eta]_\phi$)]

and cellulose), due to their (almost) negligible segment mobility. (Another problem is connected with the counter diffusion of low-d.p. coils; sometimes, it makes s_0 smaller than S_0. This paradox is explained by the definitions of s_0 and S_0; only the latter is corrected for back diffusion. The corresponding definition of s_0 would be s_0 (observed) = $s_0(1 - m_c)$, where m_c is the coil mobility. Defined in that way, it is always true that $s_0 \geqslant S_0$.)

When neither sedimentation data in the concentrated regime, nor mobility data are given, the determination of S^* is problematic. However, here, it will be shown how it can be achieved. The values of s_0 obtained will still be somewhat uncertain, but they should have gained in accuracy.

Cadoxen (cadmium hydroxide–ethylenediamine) is a solvent for unsubstituted cellulose. The first extensive study of dilute solutions of cellulose in Cadoxen was performed by Henley[20]. He showed in several ways that cellulose is as stiff in this solvent as are such cellulose derivatives as HEC in water. His findings have been verified by many other authors From his work, sedimentation data suited for Eq. 5 are shown in Table II and in Fig. 7. Only concentrations $c < c^*/2$ are represented here. As mobility data are not available, (c^*,S^*) points have to be determined directly from the sedimentation data. For each d.p. fraction, the best straight

line is drawn through the experimental points in the Figure. The desired square point is obtained where this line cuts $c = c^*$. In the case of the highest-d.p sample, only two experimental points are available in the topical concentration range In this case, the location of the square point is estimated by means of c^* and a value of S^*, as obtained *via* extrapolation from the other square points The result is adjusted by means of the expected regularity in the slopes of the initial lines through the experimental points. The result of this operation is remarkable: all square points are located on the same line as the original experimental points of the lowest-d.p fraction (The latter points are represented by the crosses in Fig 7.) According to the model proposed here, the explanation is that the very expanded cellulose coils allow free draining at the d.p. in question (d p.$_{ww}$ = 260). In such a case, $s_0 = S_0$ and is d.p.-independent (Deviations $s_0 > S_0$ are due only to drainage restrictions.) In view of the mobility profiles in Fig. 6, this is not unrealistic. According to Henley[20], the numbers (n_s) of monomers per Kuhn segment is ~20 The length of such a segment is ~100 Å, and the number N_s of Kuhn segments in the coil is 13. Furthermore, the end-to-end distance in the coils was $\langle R^2 \rangle_{ww}^{1/2} = 450$ Å. Therefore, the average distance L between the segments must exceed 100 Å. In such a case, there is very little overlap of neighboring mobility profiles Furthermore, as the total number of segments is small, the cumulative effect due to them is limited. Therefore, free draining conditions are not out of the question.

In Table II are shown the s_0 values as estimated by Henley[20], and as obtained in Fig. 7. The differences are not large, but, combined with the assumption about free draining in the lowest-d.p. sample they do give different pictures of the d.p.-dependence of s_0. Henley[20] suggested the value 0 40 for the exponent in the empirical relation

$$s_0 = \mathrm{K} \cdot \mathrm{d.p.}^{\alpha} \qquad (13)$$

It was determined from the slope of the best-fitting line in a double-logarithmic plot of data from all six cellulose samples. Fig. 8 is the corresponding plot of the data as

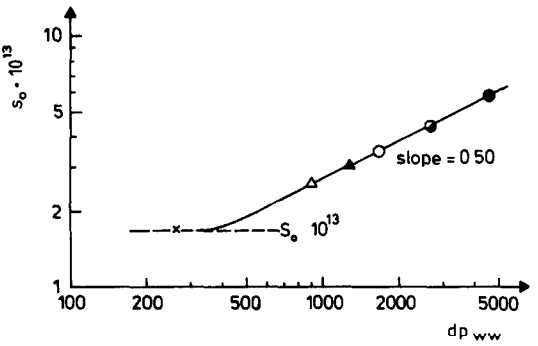

Fig 8 Double-logarithmic plot of s_0 (from Fig 7) *versus* d p of cellulose in Cadoxen (For symbols, see Table II)

obtained in Fig. 7. The plot gives $\alpha = 0.50$ when the lowest-d.p. sample is disregarded in the linear regression. (The difference in α gives quite a different theoretical view of the system[5], but will not be further commented on here.) As already discussed, the lowest-d.p. sample does not join this line. Its s_0 value is approximately equal to the value of S_0. It is expected to be d.p.-independent down to a d.p. of ~50. Below that, end effects should become increasingly important, giving rise to a decrease in s_0. An increasing counter-diffusion with decreasing d.p. will accentuate this tendency.

DISCUSSION

The present work supports many well-known facts about the D-glucans compared. Here it is shown that (1) all three polymers exist as open coils in aqueous solution (the two-phase approach of Eq. *2* is applicable); (2) the amylose segments are compact (high S_0 value, despite high friction) and heavy ($m_s = 0$, *i.e.*, the amylose chain is stiff); (3) the cellulose segments are expanded (free draining at d.p. = 260) and heavy ($m_s = 0$, the cellulose chain is also stiff); and (4) the dextran segment consists of a few monomers ($m_s = 0.14$; the chain is flexible).

The stiffness of the chains is due to rotation restrictions in the sigma bonds which link the D-glucose rings together. In the case of dextran, there are three bonds, which assure the linkage a high degree of freedom. In cellulose and amylose, there are only two sigma bonds per linkage. Thereby, the degree of freedom is considerably lessened. The restrictions are mainly caused by steric hindrance in the polymer backbones. In the case of cellulose, the steric hindrance is increased by substituents on the 2- and 3-hydroxyl groups. The restrictions also include a hydrogen bond *via* the 6-hydroxyl hydrogen atom to an adjacent monomer[21]. This hydrogen bond can exist only when the hydroxyl group is neither substituted, nor deprotonated. (For the 6-hydroxyl group, pK_a = pH in 0.50M NaOH. For the two others, pK_a = pH in M and 4M NaOH, respectively[22].

The number (n_s) of monomers in the cellulose segments is $7 < n_s < 25$. Which value n_s adopts in this range is determined by $d.s._i$ and pH, rather independent of the sort of substituent[21]. ($D.s._i$ is the degree of substitution of the *i*-hydroxyl group in the monomer.)

The effect of Cadoxen on the stiffness of the cellulose chain is not measured. However, it can be estimated by means of the data in ref. 21. If no effect is caused by complexing mechanisms in the system, the alkalinity of the solvent would make $n_s \simeq 10$. Complexing would raise this value somewhat. This estimated value is in agreement with that that Henley[20] obtained by means of viscosity and sedimentation data applied to the theory of Kuhn and Kuhn[23] ($11 \leqslant n_s \leqslant 28$).

From the estimated value $n_s > 10$ for cellulose in Cadoxen, it follows that $m_s \simeq 0$. Thus, S_0 (observed) $= S_0(1 - m_s) \simeq S_0$. In such a case, the observed value $S_0 = 1.7 \cdot 10^{-13}$ s for cellulose in Cadoxen (see Fig. 7) can be directly compared with the value $1.4 \cdot 10^{-13}$ s for HEC in water (see Table I). Cellulose in Cadoxen thus

shows approximately the same picture as HEC in water, as far as sedimentation rate *versus* friction of the segments (high friction and low sedimentation-rate) is concerned.

The difference in m_s between the polysaccharides on the one hand and polystyrene on the other reflects the much more flexible backbone of the latter. The high m_s value of p.s. ($m_s = 0.6$) corresponds to nearly free rotation in each sigma bond in the p.s. backbone (there are two such bonds per monomer). This estimate is based on the relationship

$$n_s = \frac{M(\text{solvent})}{3 \cdot M(\text{monomer}) \cdot m_s^2} \tag{14}$$

which was obtained from the thermal equilibrium conditions according to Boltzmann. The assumed moving mass of the segment (the segment itself plus one neighbor segment on each side) is $3n_sM(\text{monomer})$, and the mobility is m_s. The moving mass of a solvent molecule is $M(\text{solvent})$, and its mobility is, by definition, unity. The data in Table III show the same picture. They refer to d.p. 2000, and demonstrate a very large difference in ϕ^* (by a factor of 30) for p.s. and cellulose. The extremely low ϕ^* value of cellulose reflects the extraordinary expansion of the cellulose coil that is due to the long, rodlike segments. (An additional expansion due to swelling and excluded volume must be of marginal importance.)

It is possible to quantify the difference in ϕ^* in terms of n_s by means of the following relationships.

$$\phi^* \propto \langle R^2 \rangle_0^{-3/2} \alpha^{-3} \tag{15}$$

$$\langle R^2 \rangle_0 = N_s \cdot l_s^2 \tag{16}$$

$$N_s = \text{d.p.}/n_s \tag{17}$$

$$l_s = n_s \cdot l_m \tag{18}$$

$\langle R^2 \rangle_0^{1/2}$ is the unperturbed, end-to-end distance of the chain, α is the expansion factor, l_s is the segment length, and l_m is the length of the monomer projection on the segment axis[5]. The other n_s values were obtained by assuming n_s (cellulose) = 20, and by means of the l_m values as given in Table III. [l_m(amylose) = 1.3 Å corresponds to 1/6 of the pitch of the amylose helix[19]]

The expansion factor α is the product of an excluded volume factor and a swelling factor. In theta-solvents, the swelling factor is unity. The excluded-volume factor will only deviate from unity in very dense coils. Assuming $\alpha \simeq 1$ for both p.s. and cellulose, n_s(p.s.) is much larger as estimated in this way than *via* $\langle m_1 \rangle$. The difference is presumably due to errors in the assumptions made: $\alpha_1 = 1$, n_s(cellulose) = 20, the l_m values chosen, and the number (3) of moving segments. By means of minor changes in these values, the two estimates of n_s(p s.) would come much closer to each other

There is also another reason for the difference in the n_s(p.s.) values: $\langle m_1 \rangle$ is

measured by different techniques in the p.s. and the cellulose (HEC) systems. It was determined by means of nuclear magnetic resonance (n.m.r.) spectroscopy in the p.s. system, and with fluorescence depolarization (f.d.p.) in the HEC system. As n.m.r. decodes the motion of individual solvent molecules and f.d.p. gives the collective mobility of the group of solvent molecules surrounding the spin label, $\langle m_1 \rangle$ is higher as determined by means of n.m.r. spectroscopy. (The solvent mobility, as determined by means of f.d p., should be the more equivalent to the mobility connected with sedimentation. Also, in this case, it is the coordinated motion of a group of solvent molecules which determines the motion of the label, which is the polymer segment in this case.)

Considering the conditions for each type of n_s determination, the agreement between the polysaccharide values in Tables I and III is striking. Water is approximately a theta-solvent for amylose[24], and thermodynamically it is a good solvent for dextran. Therefore, α for dextran exceeds unity. (The value $n_s = \infty$ in Table I refers to a value of m_s which is zero within the limits of error in Fig. 4. In practice, it corresponds to a value of n_s larger than, say, 15.) The amylose value in Table III is of the same order of magnitude as $n_s = 123$, found by Banks and Greenwood[24] by means of the same type of calculation, and the value 140 ±20, obtained by a quite different method in ref. 18.

REFERENCES

1 T Svedberg and K O Pedersen, *The Ultracentrifuge,* Clarendon Press, Oxford, 1940
2 B Enoksson, *Nature (London),* 161 (1948) 934–935
3 P G de Gennes, *Scaling Concepts in Polymer Physics,* Cornell Univ Press, Ithaca, New York, 1979
4 J R Kirkwood and J Riseman, *J. Chem Phys* , 16 (1948) 565–573
5 P J Flory, *Principles of Polymer Chemistry,* Cornell Univ Press, Ithaca, New York, 1953
6 P Debye and A. M Bueche, *J Chem Phys* , 20 (1952) 1337–1338
7 Lord Rayleigh, *Philos Mag* , 37 (1919) 321–322
8 W Kuhn, *Kolloid-Z* , 68 (1934) 2–15
9 R Simha, *J Chem Phys* , 13 (1945) 188–195
10 C Wolff, *Eur Polym J* , 13 (1977) 739–741
11 H Elmgren, *J Polym. Sci , Polym Lett Ed* , 20 (1982) 57–60
12 H Elmgren, *J Polym. Sci , Polym Lett Ed* , 19 (1981) 561–565.
13 H Elmgren, *J Polym Sci , Polym Lett Ed.*, 19 (1981) 567–574
14 H Elmgren, *J Polym Sci , Polym Lett Ed* , 20 (1982) 389–396
15 B Ebert and H Elmgren, *Biopolymers,* 23 (1984) 2543–2557
16 H Elmgren, *J Polym Sci , Polym Lett Ed* , 18 (1980) 339–350
17 H Elmgren, *J Polym Sci , Polym Lett Ed* , 20 (1982) 373–374
18 H Elmgren, *Biopolymers,* 23 (1984) 2525–2541
19 R C Jordan, D A Brant, and A Cesàro, *Biopolymers,* 17 (1978) 2617–2632
20 D Henley, *Ark Kemi,* 18 (1961) 327–392
21 H Elmgren, *J Chim Phys* , 65 (1968) 206–210
22 H Elmgren, *Sven Papperstidn* , 70 (1967) 78–83
23 H Kuhn and W Kuhn, *Helv Chim Acta,* 30 (1947) 1233–1256.
24 W Banks and C T Greenwood, *Starch and its Components,* Univ Press. Edinburgh, 1975
25 B Nyström, J Roots, and R Bergman, *Polymer,* 20 (1979) 157–161
26 W Brown, P Stilbs, and R. M Johnsen, *J Polym Sci , Polym Phys Ed* , 20 (1982) 1771–1780
27 L -O Sundelöf and B Nyström, *J Polym Sci , Polym Lett Ed* , 15 (1977) 377–384
28 B Nyström, M E Moseley, P Stilbs, and J. Roots, *Polymer,* 22 (1981) 218–220
29 D Biddle, *Ark. Kemi,* 29 (1968) 553–561
30 D Biddle and S. Pardhan, *Ark Kemi,* 32 (1970) 43–53